



# Morphological Predictors of Primary Lung Cancer among Part-Solid Ground-Glass Nodules on High-Resolution CT

Hirotsugu Notsuda,<sup>1,\*</sup> Hiroki Oshio,<sup>2,\*</sup> Ken Onodera,<sup>1</sup> Takashi Hirama,<sup>1</sup>  
Yui Watanabe,<sup>1</sup> Tatsuaki Watanabe,<sup>1</sup> Takaya Suzuki,<sup>1</sup> Hisashi Oishi,<sup>1</sup>  
Hiromichi Niikawa,<sup>1</sup> Ryoko Saito-Koyama,<sup>3</sup> Masafumi Noda,<sup>1</sup> Junya Tominaga<sup>4</sup>  
and Yoshinori Okada<sup>1</sup>

<sup>1</sup>Department of Thoracic Surgery, Institute of Development, Aging and Cancer, Tohoku University, Sendai, Miyagi, Japan

<sup>2</sup>Department of Thoracic Surgery, Isawa Hospital, Mizusawa, Iwate, Japan

<sup>3</sup>Department of Pathology, National Hospital Organization, Sendai Medical Center, Sendai, Miyagi, Japan

<sup>4</sup>Department of Diagnostic Radiology, Tohoku University Hospital, Sendai, Miyagi, Japan

Recent advancements in computed tomography (CT) scanning have improved the detection rates of peripheral pulmonary nodules, including those with ground-glass opacities (GGOs). This study focuses on part-solid pure ground-glass nodules (GGNs) and aims to identify imaging predictors that can reliably differentiate primary lung cancer from nodules with other diagnoses among part-solid GGNs on high-resolution CT (HRCT). A retrospective study was conducted on 609 patients who underwent surgical treatment or observation for lung nodules. Radiological findings from pre-operative HRCT scans were reviewed and several CT imaging features of part-solid GGNs were examined for their positive predictive value to identify primary lung cancer. The proportions of the nodules with a final diagnosis of primary lung cancer were significantly higher in part-solid GGNs (91.9%) compared with solid nodules (70.3%) or pure GGNs (66.7%). Among CT imaging features of part-solid GGNs that were evaluated, consolidation-to-tumor ratio (CTR) < 0.5 (98.1%), pleural indentation (96.4%), and clear tumor border (96.7%) had high positive predictive value to identify primary lung cancer. When two imaging features were combined, the combination of CTR < 0.5 and a clear tumor border was identified to have 100% positive predictive values with a sensitivity of 40.8%. Thus we conclude that part-solid GGNs with a CTR < 0.5 accompanied by a clear tumor border evaluated by HRCT are very likely to be primary lung cancers with an acceptable sensitivity. Preoperative diagnostic procedures to obtain a pathological diagnosis may potentially be omitted in patients harboring such part-solid GGNs.

**Keywords:** computed tomography; consolidation-to-tumor ratio; ground-glass nodule; high-resolution CT; lung cancer

Tohoku J. Exp. Med., 2024 May, 263 (1), 35-42.

doi: 10.1620/tjem.2024.J016

## Introduction

Recent functional advances in computed tomography (CT) scanning have led to improved detection rates of peripheral pulmonary nodules, including those with ground-glass opacities (GGOs) (Chen et al. 2018; Ichinose et al. 2020). On high-resolution CT (HRCT), pulmonary nodules are radiologically classified into three main categories: solid

nodules, pure ground-glass nodules (GGNs), and part-solid GGNs (Henschke et al. 2021; Adams et al. 2023). Among these, small part-solid GGNs with a diameter > 1 cm are likely to be lung adenocarcinomas and a full investigation and appropriate management are recommended for patients harboring such nodules (Henschke et al. 2021). Surgical resection has been recognized as a preferred approach for treatment of such patients as long as they do not have find-

---

Received December 22, 2023; revised and accepted February 3, 2024; J-STAGE Advance online publication February 15, 2024

\*These two authors contributed equally to this work.

Correspondence: Hirotsugu Notsuda, Department of Thoracic Surgery, Institute of Development, Aging and Cancer, Tohoku University, 4-1 Seiryomachi, Aoba-ku, Sendai, Miyagi 980-8575, Japan.

e-mail: hirotsugu.notsuda.c4@tohoku.ac.jp

©2024 Tohoku University Medical Press. This is an open-access article distributed under the terms of the Creative Commons Attribution-NonCommercial-NoDerivatives 4.0 International License (CC-BY-NC-ND 4.0). Anyone may download, reuse, copy, reprint, or distribute the article without modifications or adaptations for non-profit purposes if they cite the original authors and source properly.  
<https://creativecommons.org/licenses/by-nc-nd/4.0/>

ings of mediastinal lymph node metastasis.

Although various techniques including virtual bronchoscopy, endobronchial ultrasonography with a guide sheath, and CT-guided biopsy have been used to obtain a pathological diagnosis of pulmonary nodules, their diagnostic efficacy remains suboptimal, particularly for small peripheral part-solid and pure GGNs. These diagnostic procedures are invasive and have a certain rate of complications such as pneumothorax and air embolism, and some reports have shown an association of these procedures with poor recurrence-free survival (Shimizu et al. 2006; Suzuki et al. 2015; Abe et al. 2018; Yasukawa et al. 2021). From this point of view, intra-operative diagnosis and subsequent treatment without preoperative bronchoscopy or CT-guided biopsy may be warranted in patients with part-solid GGNs when the nodule is highly likely to be lung cancer based on the CT findings.

Previous studies have demonstrated that 80.1% to 87.6% of GGNs (Henschke et al. 2002, 2013; Qiu et al., 2016; Gao et al. 2019) and 90.5% to 93.3% of part-solid GGNs (Nakata et al. 2002; Henschke et al. 2013; Hattori et al. 2016; Qiu et al. 2016) were lung adenocarcinoma. However, attempts have rarely been made to further identify morphological characteristics specific to primary lung cancer among part-solid GGNs. This retrospective study was conducted to identify reliable imaging predictors of primary lung cancer among part-solid GGNs on HRCT.

## Materials and Methods

### *Ethical approval*

Ethical approval for this study was obtained from the ethics committees of Tohoku University Hospital, and the requirement for informed consent was waived for individual patients (No. 2021-1-912-1).

### *Patients*

A retrospective study was conducted on 609 consecutive patients who were referred to our department for examination of suspected lung cancer from January 2014 to December 2018. Of these patients, 553 underwent surgical treatment, and 47 did not undergo surgery due to shrinkage or disappearance of the nodules.

### *CT scanning*

All patients underwent pre-operative HRCT. Chest images were acquired using 64-detector row CT scanners (LightSpeed VCT: GE Healthcare, Milwaukee, WI, USA, and SOMATOM Sensation Cardiac 64: Siemens Medical Systems, Erlangen, Germany). HRCT scans were performed to evaluate the entire lung with a collimation of 1-2 mm. The lung window settings included a window level of -650 Hounsfield units (HU) and a window width of 1,600 HU. GGO was defined as a misty increase in attenuation that did not obscure the underlying lung structures in the lung window setting, while consolidation was defined as an increase in attenuation that obscured the underlying structures

(Hansell et al. 2008). The solid tumor size was determined as the maximum dimension of the solid component of the lung windows, excluding GGO. The consolidation-to-tumor ratio (CTR) was defined as the maximum dimension of consolidation on the lung window setting divided by the maximum dimension of the tumor on the lung window setting.

### *Definition of morphological classifications of pulmonary nodules*

Based on the radiological findings on HRCT, pulmonary nodules were divided into three groups: solid nodules, part-solid GGNs, and pure GGNs (Fig. 1A) (Henschke et al. 2002). A solid nodule was defined as those without GGO component, a pure GGN was defined as those having only a GGO component without a consolidation component, and a part-solid GGN was defined as those with both a GGO component and a consolidation component. The location of the nodule was classified into 2 categories, peripheral and central. Peripheral nodules were defined as those located in the outside third of the distance to the lung surface from the hilum portion.

The morphological classification of part-solid GGNs were further determined based on tumor shape, the presence of pleural indentation, and the status of the tumor border. Tumor shape was divided into three categories: round/oval, lobulated/polygonal, or irregular (Fig. 1B). The classification of the tumor border was determined based on the clarity (clear or unclear) of the border between the GGO and lung parenchyma (Fig. 1C).

All radiological findings were reviewed by at least two radiologists for all cohorts.

### *Final diagnosis*

The final diagnosis of the pulmonary nodules was determined by pathological diagnosis in the patients who underwent lung resection. All resected specimens were formalin-fixed and stained with hematoxylin and eosin using routine procedures. Two experienced pathologists reviewed the surgical specimens. The TNM classification was performed according to the Union for International Cancer Control and the American Joint Committee on Cancer staging system (8th edition). Histopathological analyses were conducted according to the WHO criteria (3rd edition).

Nodules which showed an obvious shrinkage or disappearance during observation were defined as benign tumors and the final diagnoses were clinically assigned.

### *Statistical analysis*

Data were expressed as mean  $\pm$  standard deviation (SD) and absolute numbers. The Wilcoxon test and Fisher's exact test were used to compare the background characteristics between patient groups for continuous and categorical variables, respectively. P values of  $< 0.05$  were considered to be statistically significant. All statistical analyses were conducted using JMP Pro 16 (SAS Institute Inc., Cary, NC, USA).

## Results

### Characteristics of patients with solid nodules, part-solid GGNs, and pure GGNs

Out of the 609 pulmonary nodules, 431 (70.8%) were solid nodules, 136 (22.3%) were part-solid GGNs, and 42 (6.9%) were pure GGNs (Table 1). Patients with solid nodules were more likely to be men compared to patients in the

other two categories (proportion of men: 62.9%, 44.1%, and 50.0% in patients with solid nodules, part-solid GGNs, and pure GGNs, respectively). The mean age of patients in each category was  $66.8 \pm 10.0$ ,  $68.6 \pm 8.07$ , and  $67.6 \pm 7.7$  years, respectively. Patients with solid nodules had a significantly higher Brinkman index (BI) compared to patients in the other two categories (BI:  $552 \pm 573$ ,  $274 \pm 447$ , and  $235 \pm 328$  in patients with solid nodules, part-solid GGNs,

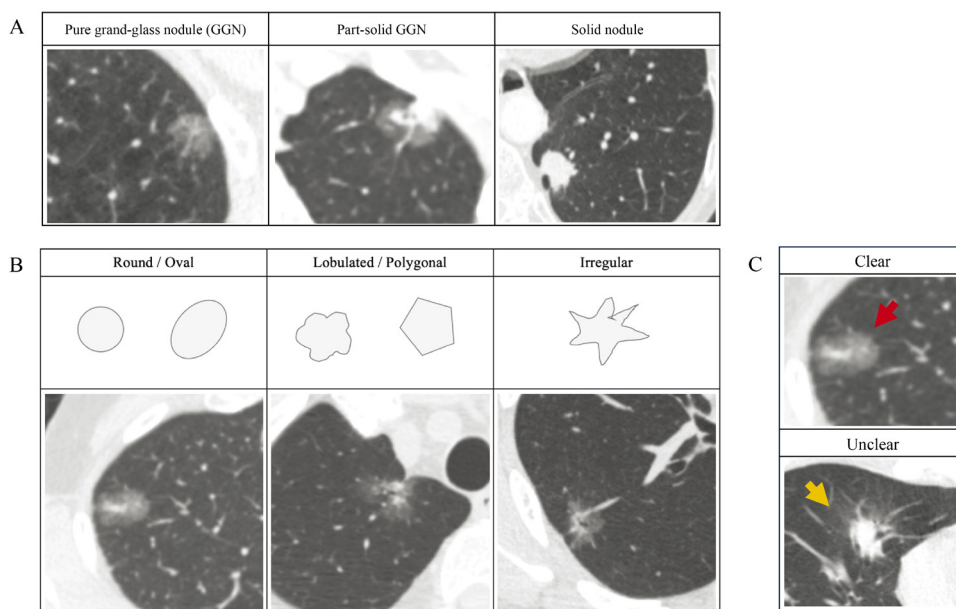


Fig. 1. Morphological classifications of pulmonary nodules.

(A) Representative computed tomography images of pulmonary nodules. (B) Definition of the tumor shape. (C) The tumor border of part-solid ground-glass nodules (GGNs).

Table 1. Clinicopathological characteristics of patients with lung nodules on CT.

	Solid nodule (n = 431)	Part-solid GGN (n = 136)	Pure GGN (n = 42)	P value
Age, years, mean $\pm$ SD	$66.8 \pm 10.0$	$68.6 \pm 8.07$	$67.6 \pm 7.7$	0.156
Sex, Male, n (%)	*271 (62.9)	60 (44.1)	21 (50)	0.03
Location of main tumor, peripheral, n (%)	238 (55.2)	67 (49.3)	26 (61.9)	0.28
Brinkman index, mean $\pm$ SD	*552 $\pm$ 573	274 $\pm$ 447	235 $\pm$ 328	< 0.001
Tumor size, mean $\pm$ SD on CT, mm	26 $\pm$ 17	28 $\pm$ 15	*18 $\pm$ 8	0.001
SUVmax, mean $\pm$ SD	*6.88 $\pm$ 5.21	2.74 $\pm$ 2.16	1.28 $\pm$ 0.80	< 0.001
Treatment				
Surgery, n (%)	394 (91.4)	130 (95.5)	*30 (71.4)	< 0.001
Lobectomy	263 (66.8)	105 (81.4)	9 (30.0)	
Sublobar resection	128 (32.5)	23 (17.8)	21 (70.0)	
Pathology, n (%)				
Primary lung cancer	303 (70.3)	*125 (91.9)	28 (66.7)	< 0.001
Lung adenocarcinoma	195 (45.2)	*123 (90.4)	28 (66.7)	< 0.001
Metastatic lung tumor	66 (15.3)	2 (1.5)	0 (0)	
Benign tumor	33 (7.7)	3 (2.2)	2 (4.8)	
Spontaneous regression, n (%)	29 (6.7)	6 (4.4)	12 (28.5)	

\*Significant difference between the other two groups.

GGN, ground-glass nodule; SUVmax, maximum standardized uptake value.

and pure GGNs, respectively). The maximum tumor sizes of pure GGNs were smaller compared to those of the other two categories (maximum tumor size:  $26 \pm 17$  mm,  $28 \pm 15$  mm, and  $18 \pm 8$  mm in solid nodules, part-solid GGNs, and pure GGNs, respectively). PET SUVmax values were  $6.88 \pm 5.21$ ,  $2.74 \pm 2.16$ , and  $1.28 \pm 0.80$ , respectively, and significant differences were observed among the three categories. There were no significant differences in tumor localization (peripheral or central) among the three categories.

*The proportion of a final diagnosis of primary lung cancer in the three categories*

The proportions of the final diagnoses of primary lung

cancer in the solid nodules, part-solid GGNs, and pure GGNs were 70.3% (303/431), 91.9% (125/136), and 66.7% (28/42), respectively. Part-solid GGNs were significantly more likely to have a final diagnosis of primary lung cancer compared to the other two categories. The proportions of lung adenocarcinoma cases within the solid nodules, part-solid GGNs, and pure GGN group were 45.2% (195/431), 90.4% (123/135), and 66.7% (28/42), respectively (Table 1, Fig. 2).

*Clinical and pathological characteristics of patients with part-solid GGNs*

Among the 136 patients with part-solid GGNs, 125

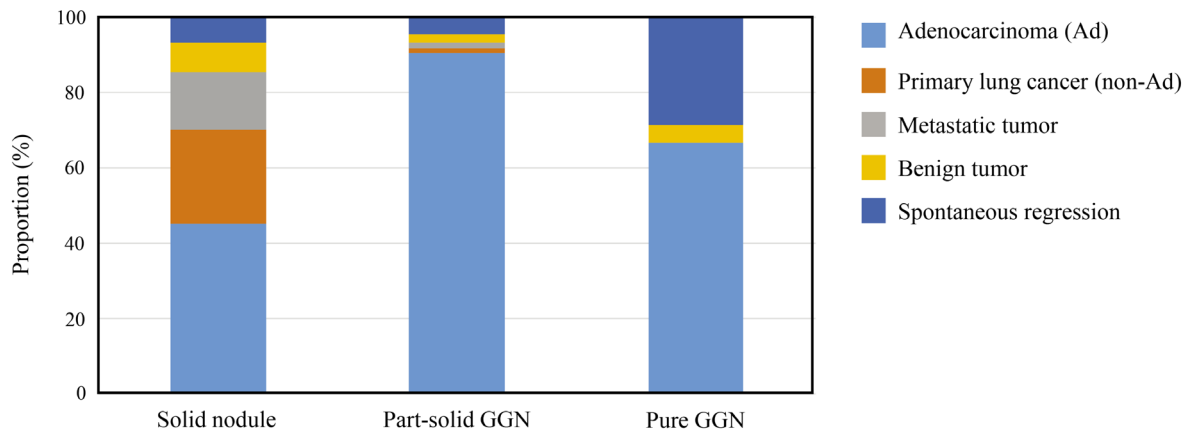


Fig. 2. Proportions of diseases in the solid nodules, part-solid ground-glass nodules (GGNs), and pure GGNs. The proportions of primary lung cancer cases within the solid nodules, part-solid GGNs, and pure GGNs were 70.3%, 91.9%, and 66.7%, respectively.

Table 2. Clinicopathological characteristics of patients with part-solid ground-glass nodule (GGN) on CT.

	Primary lung cancer (n = 125)	Non-primary lung cancer (n = 11)	P value
Age, years, mean $\pm$ SD	69 $\pm$ 8.1	69 $\pm$ 7.7	0.810
Sex, male, n (%)	52 (41.6)	8 (72.7)	0.046
Location of nodules, peripheral, n (%)	61 (48.8)	7 (63.6)	0.294
Brinkman index, mean $\pm$ SD	261 $\pm$ 435	429 $\pm$ 560	0.233
Tumor size, mean $\pm$ SD on CT, mm	29.6 $\pm$ 14.9	31.3 $\pm$ 12.1	0.719
SUVmax, mean $\pm$ SD	2.64 $\pm$ 2.02	3.59 $\pm$ 3.19	0.072
Treatment, n (%)			
Surgery	125 (100)	5 (45.5)	< 0.001
Lobectomy	104 (83.2)	2 (18.2)	
Sublobar resection	20 (16.0)	3 (27.3)	
Pathology, n (%)			
Lung adenocarcinoma	123 (98.4)	0 (0)	
Metastatic lung tumor	0 (0)	2 (2.2)	
Benign tumor	0 (0)	3 (2.2)	
Spontaneous regression, n (%)	0 (0)	6 (4.4)	
Mean tumor size (range) on pathology, mm	23.9 $\pm$ 11.1 (8-64)	N/A	
Mean invasive tumor size (range) on pathology, mm	17.4 $\pm$ 10.9 (2-52)	N/A	

SUVmax, maximum standardized uptake value; N/A, not applicable.

patients were finally diagnosed with primary lung cancer, while 11 patients had other diseases. The final diagnosis was determined by a pathological examination of the resected specimens in all cases of primary lung cancer. Among 11 non-primary lung cancer cases, 5 cases underwent surgery leading to a pathological diagnosis and the final diagnosis of the remaining 6 cases were determined clinically. There were no significant differences in tumor diameter, SUVmax, or tumor localization between the nodules with a final diagnosis of primary lung cancer and the others. Of 125 primary lung cancer cases, the pathological diagnosis of 123 cases was adenocarcinomas (98.4%). The final diagnosis of the 11 non-primary lung cancer cases consisted of 9 benign nodules and 2 metastatic tumors (Table 2).

#### *Imaging characteristics of part-solid GGNs diagnosed as primary lung cancer and other diseases*

The CTR of part-solid GGNs with a final diagnosis of primary lung cancer was smaller compared to those with other diagnoses ( $0.60 \pm 0.25$  vs.  $0.81 \pm 0.22$ ,  $P = 0.005$ ) (Table 3). When we set an axis of the CTR at 0.5, a higher percentage of primary lung cancer nodules had a CTR of

0.5 or less (41.0%) compared to those diagnosed with other diseases (9.1%) ( $P = 0.23$ ). Regarding the shapes of the part-solid GGNs, proportions of round/oval or lobulated/polygonal nodules tended to be higher in primary lung cancer (20% vs. 9.1% and 24.9% vs. 0%, respectively), while the shapes of 10 of 11 nodules (90.9%) in non-primary lung cancer cases were irregular. Pleural indentation was more likely to be identified in primary lung cancer nodules (64.8%) compared to non-primary lung cancer nodules (36.4%). A clear tumor border was also more frequently seen in lung cancer nodules (95.2%) compared to non-primary lung cancer nodules (36.4%) (Table 3). To summarize,  $CTR < 0.5$ , pleural indentation and a clear tumor border appeared to be useful in identifying primary lung cancer among part-solid GGNs. We then calculated the positive predictive values for these three imaging features (Table 4). All imaging features showed high positive values to predict primary lung cancer over 95%. Furthermore, when two of the three features were combined, a  $CTR < 0.5$  and a clear tumor border was identified to have a 100% positive predictive value with a sensitivity of 40.8%. The combination of  $CTR < 0.5$  and pleural indentation also showed a 100% positive predictive value but the sensitivity was 21.6%

Table 3. CT imaging features of patients with part-solid ground-glass nodules (GGNs).

	Primary lung cancer (n = 125)	Non-primary lung cancer (n = 11)	P value
Tumor size, mean $\pm$ SD (range) on CT, mm	29.6 $\pm$ 14.9 (8-115)	31.3 $\pm$ 12.1 (15-52)	0.719
Mean solid nodule size (range) on CT, mm	18.1 $\pm$ 13.7 (3-53)	26.5 $\pm$ 15.0 (13-52)	0.054
CTR	0.60 $\pm$ 0.25	0.81 $\pm$ 0.22	0.005
0 < CTR $\leq$ 0.5, n (%)	51 (41.0)	1 (9.1)	0.023
Shape of part-solid GGNs, n (%)			
Round/oval	25 (20)	1 (9.1)	
Lobulated/polygonal	31 (24.9)	0 (0)	
Irregular	69 (55.2)	10 (90.9)	0.049
Pleural indentation, n (%)	81 (64.8)	3 (27.3)	0.009
Clear tumor border, n (%)	119 (95.2)	4 (36.4)	< 0.001

CTR, consolidation-to-tumor ratio.

Table 4. Positive predictive value of CT imaging features for primary lung cancer with part-solid ground-glass nodules (GGNs).

	Primary lung cancer (n = 125)	Non-primary lung cancer (n = 11)	Positive predictive value (%)	P value
CTR, 0 < CTR $\leq$ 0.5, n (%)	51 (41.0)	1 (9.1)	98.1	0.023
B. Pleural indentation, n (%)	81 (64.8)	3 (27.3)	96.4	0.009
C. Clear tumor border, n (%)	119 (95.2)	4 (36.4)	96.7	< 0.001
A and B	27 (21.6)	0 (0)	100	0.085
A and C	51 (41.0)	0 (0)	100	0.007
B and C	79 (63.2)	1 (9.1)	98.8	0.001

CTR, consolidation-to-tumor ratio.

(Table 4). Thus, we propose that the combination of CTR < 0.5 and clear tumor border is a highly reliable imaging feature with an acceptable sensitivity to predict lung cancer among part-solid GGNs (Fig. 3).

#### Imaging characteristics of non-primary lung cancer nodules

Among 11 part-solid GGNs with a final diagnosis of non-primary lung cancer, nodules with CTR > 0.5 accounted for 10 cases (90.9%). These cases (90.9%) also had an irregular shape and 7 cases (63.6%) showed an unclear tumor border (Table 5, Fig. 4A-D). These results indicated that the imaging features to suspect non-primary lung cancer nodule included CTR > 0.5, irregular shape and an unclear tumor border.

## Discussion

The principal finding of this study is that part-solid GGNs with a CTR < 0.5 accompanied by a clear tumor border evaluated by HRCT are very likely to be primary lung cancers. On the other hand, the imaging features of part-solid GGNs with a final diagnosis other than primary lung cancer included CTR > 0.5 (90.9%), irregular shape (90.9%) and unclear tumor border (63.6%).

In the present study, 28 of 42 (66.7%) pure GGNs and 303 out of 431 (70.3%) solid nodules were finally diagnosed as primary lung cancers. In marked contrast, a final diagnosis of 125 of 136 part-solid GGNs (91.9%) was primary lung cancers, and a pathological diagnosis of the most

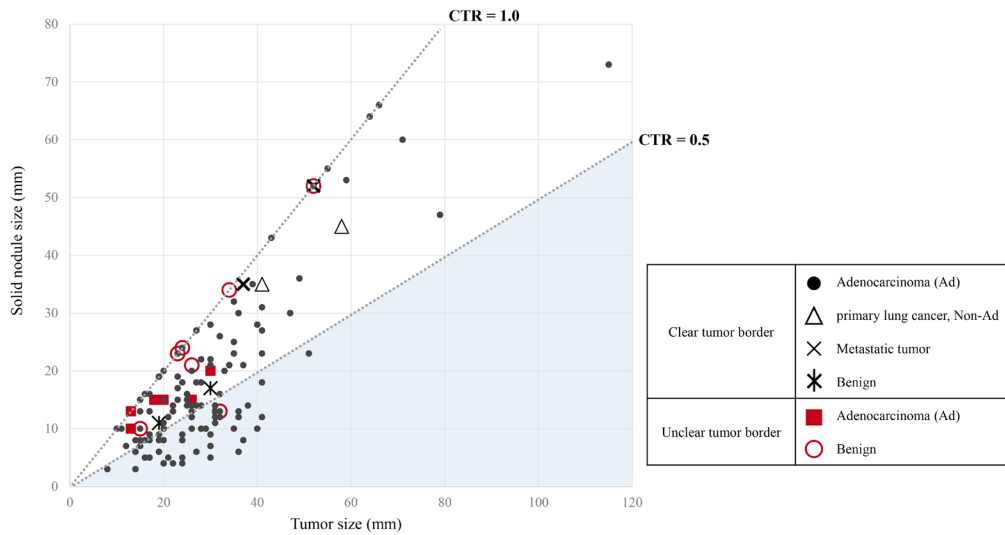


Fig. 3. The plots showing the relationship between consolidation-to-tumor ratio (CTR) (Y axis) and tumor size (X axis), and final diagnosis of lung tumors.

Lung adenocarcinomas are represented by ●, lung cancers other than adenocarcinoma by △, metastatic tumors by ×, and benign lesions by \*. Part-solid ground-glass nodules (GGNs) with a CTR of 0.5 or less, except for one tumor, were diagnosed as primary lung cancer.

Table 5. Morphological characteristics and history of 11 cases diagnosed with non-primary lung cancer.

Case Number	Maximum tumor size (mm)	CTR	Pleural indentation	Tumor border	Shape of tumor	Treatment	Diagnose
1	32	0.41	No	Unclear	Irregular	Observation	Inflammation
2	30	0.57	Yes	Clear	Irregular	Observation	Inflammation
3	19	0.58	No	Clear	Irregular	Observation	Inflammation
4	15	0.67	No	Unclear	Irregular	Wedge resection	Fibrous scar
5	26	0.81	Yes	Unclear	Irregular	Observation	Inflammation
6	37	0.95	No	Clear	Round/oval	Wedge resection	Metastatic tumor
7	52	1.0	No	Clear	Irregular	Lobectomy	Metastatic tumor
8	23	1.0	No	Unclear	Irregular	Lobectomy	Fibrous scar
9	24	1.0	Yes	Unclear	Irregular	Observation	Inflammation
10	34	1.0	No	Unclear	Irregular	Observation	Inflammation
11	52	1.0	No	Unclear	Irregular	Wedge resection	Granuloma

CTR, consolidation-to-tumor ratio.

of them (123 of 125) was lung adenocarcinoma (90.4%). These results of the present study were consistent with those in previous studies. Gao and Henschke et al. reported that 80.1% to 87.6% of surgically resected GGNs were lung adenocarcinoma (Henschke et al. 2002, 2013; Qiu et al. 2016; Gao et al. 2019). Hattori and Nakata et al. reported that 90.5% to 93.3% of part-solid GGNscases were found to be lung adenocarcinoma (Nakata et al. 2002; Henschke et al. 2013; Hattori et al. 2016; Qiu et al. 2016). However, it should be noted that 10 to 20% of GGNs and 10% of part-solid GGNs were finally diagnosed as other diseases and a large part of these nodules were benign, at least in our study. Thus, we intended to identify the imaging predictors of characteristic primary lung cancer among part-solid GGNs in the present study.

The present study demonstrated that  $CTR < 0.5$  has the highest positive predictive value to identify primary lung cancer among several imaging features of part-solid GGNs. We set an axis of  $CTR < 0.5$  based on the results of the present study (Fig. 3) in order to ease the clinical application. Other imaging features, pleural indentation and clear tumor border also have high positive predictive value and, when two imaging features were combined, the combination of  $CTR < 0.5$  and clear tumor border was identified to have 100% of positive predictive values with a sensitivity

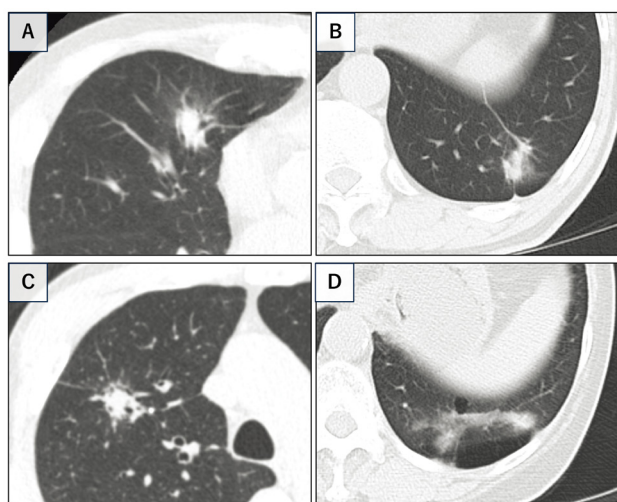


Fig. 4. Representative computed tomography images of part-solid ground-glass nodules diagnosed with non-primary lung cancer.

(A) A part-solid ground-glass nodule (GGN) with a consolidation-to-tumor ratio (CTR) of 0.41 and an unclear tumor border, which disappeared during follow-up (Case number 1 in Table 5). (B) A part-solid GGN with a CTR of 0.5, an unclear tumor border and an irregular shape, which disappeared during follow-up (Case number 4 in Table 5). (C) A part-solid GGN with a CTR of 1.0, an unclear tumor border and an irregular shape, which was diagnosed as a fibrous scar after lobectomy (Case number 8 in Table 5). (D) A part-solid GGN with a CTR of 1.0, an unclear tumor border and an irregular shape, which was diagnosed as a granuloma after pulmonary wedge resection (Case number 11 in Table 5).

of 40.8%. Thus, we conclude that this combination of  $CTR < 0.5$  and clear tumor border is a highly reliable imaging feature to predict lung cancer with an acceptable sensitivity among part-solid GGNs. To our knowledge, this is the first study that incorporates a clear tumor border into the imaging criteria to identify primary lung cancer on HRCT.

The biological background of why adenocarcinoma represents a feature of  $CTR < 0.5$  and clear tumor border was not known with the results of the present study. However, we speculate that the border of GGO of adenocarcinoma on HRCT tends to be clear because it represents the border between two distinctly different tissues, adenocarcinoma with a lepidic growth and the normal lung tissue. In contrast, GGO around inflammatory nodules probably includes various degrees of inflammation which may show a gradient from the center of the nodules to the periphery. This may lead to a relatively small area of GGO with an unclear border of the inflammatory nodules.

There are several advantages for omitting examinations to obtain preoperative pathological diagnosis of lung nodules. It may reduce the period between the first referral to surgery and the medical cost will be decreased as well. Complications associated with pre-operative bronchoscopy and CT are also avoided. Intra-operative diagnosis by frozen specimens may prolong the operation time and increase some medical costs, but the benefits of omitting preoperative examinations would well compensate for it. According to the result of the present study, we propose that pre-operative diagnostic procedures including bronchoscopy and CT-guided biopsy may be omitted in patients with part-solid GGNs with a  $CTR < 0.5$  accompanied by a clear tumor border evaluated by HRCT.

This study has several limitations. This was a single center retrospective study. All patients included in this study were those referred to our surgical department and they may be a specific population with a high probability of lung cancer. The assessment of the morphological characteristics of the nodule relied on subjective assessments by clinicians although 2 experienced radiologists reviewed all HRCTs.

In conclusion, this study demonstrated that part-solid GGNs with a  $CTR < 0.5$  accompanied by a clear tumor border evaluated by HRCT are very likely to be primary lung cancers with an acceptable level of sensitivity. Preoperative diagnostic procedures to obtain pathological diagnosis may potentially be omitted in patients harboring such part-solid GGNs, although this hypothesis must be tested by prospective studies to provide solid evidence.

#### Author Contributions

Conceptualization: H.N., Y.O. and J.T.; Pathological analysis: R.K., H.N. and H.O.; Radiological analysis: J.T., H.N. and H.O.; Formal analysis and investigation: K.O., T.H., Y.W., T.W., T.S., H.O., H.N., H.N. and H.O.; Writing-original draft preparation: H.N.; Writing-review and Editing: T.H. and M.N.; Supervision: Y.O.

### Conflict of Interest

The authors declare no conflict of interest.

### References

- Abe, J., Okazaki, T., Kikuchi, N., Takahashi, S., Sakurada, A. & Okada, Y. (2018) Preoperative bronchoscopic cancer confirmation does not increase risk of recurrence in stage I A non-small cell lung cancer. *Gen. Thorac. Cardiovasc. Surg.*, **66**, 284-290.
- Adams, S.J., Stone, E., Baldwin, D.R., Vliegenthart, R., Lee, P. & Fintelmann, F.J. (2023) Lung cancer screening. *Lancet*, **401**, 390-408.
- Chen, D., Dai, C., Kadeer, X., Mao, R., Chen, Y. & Chen, C. (2018) New horizons in surgical treatment of ground-glass nodules of the lung: experience and controversies. *Ther. Clin. Risk Manag.*, **14**, 203-211.
- Gao, F., Sun, Y., Zhang, G., Zheng, X., Li, M. & Hua, Y. (2019) CT characterization of different pathological types of subcentimeter pulmonary ground-glass nodular lesions. *Br. J. Radiol.*, **92**, 20180204.
- Hansell, D.M., Bankier, A.A., MacMahon, H., McLoud, T.C., Muller, N.L. & Remy, J. (2008) Fleischner Society: glossary of terms for thoracic imaging. *Radiology*, **246**, 697-722.
- Hattori, A., Matsunaga, T., Takamochi, K., Oh, S. & Suzuki, K. (2016) Oncological characteristics of radiological invasive adenocarcinoma with additional ground-glass nodules on initial thin-section computed tomography: comparison with solitary invasive adenocarcinoma. *J. Thorac. Oncol.*, **11**, 729-736.
- Henschke, C.I., Yankelevitz, D.F., Mirtcheva, R., McGuinness, G., McCauley, D. & Miettinen, O.S.; IELCAP Group (2002) CT screening for lung cancer: frequency and significance of part-solid and nonsolid nodules. *AJR Am. J. Roentgenol.*, **178**, 1053-1057.
- Henschke, C.I., Yip, R., Shaham, D., Zulueta, J.J., Aguayo, S.M., Reeves, A.P., Jirapatnakul, A., Avila, R., Moghanaki, D. & Yankelevitz, D.F.; I-ELCAP Investigators (2021) The regimen of computed tomography screening for lung cancer: lessons learned over 25 years from the International Early Lung Cancer Action Program. *J. Thorac. Imaging*, **36**, 6-23.
- Henschke, C.I., Yip, R., Yankelevitz, D.F. & Smith, J.P.; International Early Lung Cancer Action Program Investigators\* (2013) Definition of a positive test result in computed tomography screening for lung cancer: a cohort study. *Ann. Intern. Med.*, **158**, 246-252.
- Ichinose, J., Kawaguchi, Y., Nakao, M., Matsuura, Y., Okumura, S., Ninomiya, H., Oikado, K., Nishio, M. & Mun, M. (2020) Utility of maximum CT value in predicting the invasiveness of pure ground-glass nodules. *Clin. Lung Cancer*, **21**, 281-287.
- Nakata, M., Saeki, H., Takata, I., Segawa, Y., Mogami, H., Mandai, K. & Eguchi, K. (2002) Focal ground-glass opacity detected by low-dose helical CT. *Chest*, **121**, 1464-1467.
- Qiu, Z.X., Cheng, Y., Liu, D., Wang, W.Y., Wu, X., Wu, W.L. & Li, W.M. (2016) Clinical, pathological, and radiological characteristics of solitary ground-glass opacity lung nodules on high-resolution computed tomography. *Ther. Clin. Risk Manag.*, **12**, 1445-1453.
- Shimizu, K., Ikeda, N., Tsuboi, M., Hirano, T. & Kato, H. (2006) Percutaneous CT-guided fine needle aspiration for lung cancer smaller than 2 cm and revealed by ground-glass opacity at CT. *Lung Cancer*, **51**, 173-179.
- Suzuki, K., Watanabe, S., Mizusawa, J., Moriya, Y., Yoshino, I., Tsuboi, M., Mizutani, T., Nakamura, K., Tada, H. & Asamura, H.; Japan Lung Cancer Surgical Study Group (JCOG LCSSG) (2015) Predictors of non-neoplastic lesions in lung tumours showing ground-glass opacity on thin-section computed tomography based on a multi-institutional prospective study<sup>†</sup>. *Interact. Cardiovasc. Thorac. Surg.*, **21**, 218-223.
- Yasukawa, M., Kawaguchi, T., Kimura, M., Tojo, T. & Taniguchi, S. (2021) Implications of preoperative transbronchial lung biopsy for non-small cell lung cancer less than 3-cm. *In Vivo*, **35**, 1027-1031.